Caryologia

International Journal of Cytology, Cytosystematics and Cytogenetics

OPEN ACCESS

Intracellular and extracellular green synthesis of silver nanoparticles using *Desmodesmus* sp.: their Antibacterial and antifungal effects

Betül Yilmaz Öztürk

Eskişehir Osmangazi University Central Research Laboratory Application And Research Center (ARUM), 26480 Eskişehir, Turkey
E mail: byozturk@ogu.edu.tr. ORCID: 0000-0002-1817-8240

Abstract. In this study aim was to perform green synthesis of synthesis silver nanoparticles (LAC-AgNPs, RAE-AgNPs and BAE-AgNPs) by using *Desmodesmus* sp., intracellular and extracellular synthesis methods and to compare the obtained products with physicochemical characterization techniques. The structural, morphological and optical properties of the synthesized nanoparticles were characterized using UV-Vis spectroscopy, TEM, SEM-EDS, FTIR, DLS and zeta potential. These results clearly show that silver nanoparticles (AgNPs) could be synthesized in different sizes and stabilities with various biological materials obtained from *Desmodesmus* sp. LAC-AgNPs had size of 10-30 nm, RAE-AgNPs had size of 4-8 nm and BAE-AgNPs had size of 3-6 nm. Also, the antibacterial activity of silver nanoparticles synthesized as intracellular and extracellular showed a strong antibacterial effect against pathogens such as *Salmonella* sp. and *Listeria monocytogenes*. Additionally, they have effective antifungal activity against *Candida parapsilosis*. The broth microdilution method was used for examining antibacterial antifungal effect of synthesis AgNPs. The minimum inhibitory concentration against *Salmonella* sp., *Listeria monocytogenesis* and *Candida parapsilosis* were recorded as 3,125 μl, 1,5625 μl and 0,78125 μl synthesis AgNPs, respectively. As a result, it has thought that different sizes of synthesis AgNPs may have a great potential for biomedical applications.

Keywords. Green synthesis, nanoparticle, algae, antimicrobial, *Desmodesmus* sp.

INTRODUCTION

In nanotechnology studies, the most attract attention topics is the synthesis of nanoparticles (NPs) with strong potency in different sizes and shapes or by using various variables. For example, metal NPs. The area of use for metal NPs are very broad. Even silver NPs alone are used in countless areas with optics, electronics, catalysis, home furnishings and extensive medical applications, and the annual production is estimated to be hundreds of tons worldwide (Ge et al. 2014).

Synthesis of nanomaterials containing noble metal requires alternative strategies because of their high cost. Green synthesis or green chemical synthesis leads the list of these strategies and here the target is a biological synthesis of nanomaterial and to obtain products with positive effects in terms of the environment (Sondi et al. 2000). Green synthesis has preferred because of the high costs of materials used in conventional chemical methods and due to the toxic substances released into the environment. Because the toxic effect of nanoparticles is proven in many studies on aquatic organisms in particular. For example, studies on algae (Dağlıoğlu and Öztürk 2016; Dağlıoğlu and Öztürk 2018; Öztürk and Dağlıoğlu 2018) have shown that aquatic invertebrates (*Artemia salina*) (Dağlıoğlu et al. 2016a), terrestrial invertebrates, honey bee (*Apis mellifera*) (Özkan et al. 2016), aquatic plants (*Lemna minor* and *Myriophyllum spicatum*) (Dağlıoğlu and Türkiş 2017a, b). Nevertheless, it more attracts the attention of researchers for the production of metal nanoparticles because of its low cost, environmental friendliness, and simple approach. In the green synthesis does not use reducing agents like sodium borohydride ($NaBH_4$) used in chemical synthesis (Kozma et al. 2015). These reducing agents are both expensive and may produce oxidized boron species bound to NPs after synthesis. As a result the commercially produced NPs are not appropriate for biological applications. NPs produced by green synthesis are of great importance in terms of environmentally friendly production processes and low costs. Many organisms or a variety of extracts produced by them may be used in the green synthesis process bacteria (Joerger et al. 2000), plant (Khatami et al. 2018a), fungi (Boroumand et al. 2015) and algae (Singh et al. 2013).

Algae will have a great platform for products to be used for various purposes over the next few years has a long-term sustainable potential, especially in the production of food and liquid fuels (Koothari et al. 2017). For this reason algae are commonly chosen for green synthesis because their structures are a rich source of biologically active compounds like chlorophyll, carotenoids, astaxanthin, phenol, flavonoid, protein, vitamin and minerals (Faulker 2000). Additionally, these phytochemical materials are each effective metal reducing agents and their structures contain agents ensuring that hydroxyl, carboxyl, and amino functional groups coat metal NPs (Annamalia and Nallamuthu 2015). It has been supported by various literatures that NPs synthesis can be carried out by using various algae. For example, Kannan et al. (2013) performed AgNP synthesis with extraction from *Chaetomorpha linum* species. The researchers succeeded in synthesizing spherical NPs with nearly 30 nm size without using synthetic reactives. Barwal et al. (2011) used a *Chlamydomonas reinhardtii* model and focused on understanding the role of a variety of cellular proteins in the synthesis and coating of silver NPs. Prasad et al. (2013) studied the extract of the brown algae *Cystophora moniliformis* species and reported that the sizes of NPs may change linked to temperature. Studies mainly use marine macroalgae with insufficient numbers of studies about microalgae.

It has been known for many years that silver (Ag) is an antimicrobial agent and it draws much attention due to its application in fields such as colloidal Ag, catalysis and water purification. It is reported that using AgNP may purify drinking water (Pradeep 2009). Furthermore, the effect of Ag NPs size variability on antibacterial properties has been a matter of interest. As a result, researchers who have successfully achieved green synthesis have simultaneously assessed the antibacterial and antifungal effects on a variety of microorganisms (like bacteria and yeast) (Govindaraju et al. 2009; Rajeshkumar et al. 2014; Salari et al. 2016; Suriya et al. 2012).

Our aim is to use the microalgae *Desmodesmus* sp., which can easily be produced in a laboratory environment, to compare synthesis using both intracellular and extracellular routes. For this, the differences between NPs forming under the same conditions were determined using characterization techniques like UV-Vis, TEM, SEM-EDS, FTIR, DLS and zeta potential. At the same time, antibacterial effects of synthesized NPs on bacterial strains of important food pathogens such as *Salmonella* sp. and *Listeria monocytogenesis* were investigated. Additionally, the antifungal effect on the human pathogen of *Candida parapsilosis* species was investigated.

MATERIAL AND METHOD

Algae Culture

The test organism used in our study, *Desmodesmus* sp. (KR261937)*,* was taken from the algae culture collection of Selçuk University Hydrobiology Laboratory. Algae taken from stock cultures were transferred to the fluid BG-11 medium ($NaNO_3$, 15; K_2HPO_4, 0.4; $MgSO_4·7H_2O$, 0.75; $CaCl_2·2H_2O$, 0.36; citric acid, 0.06; iron(III) ammonium citrate, 0.06; Na_2-EDTA, 0.01; Na_2CO_3, 0.2 g/L, 1 mL; trace elements solution, (H_3BO_3, 61; $MnSO_4·H_2O$, 169; $ZnSO_4 ·7H_2O$, 287; $CuSO_4·5H_2O$, 2.5; $(NH_4)_6Mo_7O_{24}·4H_2O$, 12.5 mg/L) in accordance with the procedure stated in Rippka (1988). The microalgae were transferred to 250 ml erlenmeyer flask and left to proliferate under sterile conditions. The cultures were

left under 3000 lux fluorescent light appropriate for photosynthesis for 12 hours light and 12 hours darkness, at 28±2 °C degrees, and 120 rpm for 15-20 days. When algae passed the log phase stage, cells were centrifuged at 1000 rpm and the biomass was obtained. All chemicals used in this study were analytical quality.

Intracellular AgNP synthesis using live algae cells

Silver nitrate (AgNO$_3$, ≥99.0%; Sigma-Aldrich) was prepared in 100 mM stock solution. Microalgae passing the logarithmic phase were counted with the automatic cell counting device (LUNA-II™ Automated Cell Counter, South). Using LUNA ™ Cell counting slides, counting and viability of cells were determined with trypan blue. Afterwards, live algae cells (LAC) were harvested by centrifugation at 4000 rpm for 20 minutes at 4 °C. The culture filtrate was removed and the pelleted biomass was washed with sterile deionized water to remove foreign absorbed material. The washing procedure was repeated five times and the washed biomass was brought to suspension again in distilled water. The suspension of algal biomass had 5mM AgNO$_3$ added the from stock solution. In the control setup, AgNO$_3$ was not added to the algal biomass. Cultures were incubated at 28 °C under similar conditions to those stated above for 72 hours. Intracellular Ag NPs (LAC-AgNPs) synthesis from LAC was completed. After the reaction, the biomass was separated by the centrifuge and stored at -20 °C until characterization.

Extracellular synthesis of AgNP

Two different algal extracts were obtained using Desmodesmus sp. for the extracellular synthesis of AgNP. These extracts were raw algal extract (RAE) and boiled algal extract (BAE).

Preparation of raw and boiled algae extracts

For the preparation of RAE extract, 3.0 g (wet weight) algal biomass was suspended in 20 ml of deionized water for 5 days. At the end of the 5th day, it was centrifuged at 7000 rpm for 20 minutes. The supernatant (raw algal extract) was separated from cells and prepared for extraction. To begin the reaction, the final concentration of 5 mM AgNO$_3$ was added. After this procedure, continuous mixing began. Later the mixing procedure, a colloidal structure was obtained and after this process repeated centrifugation was completed at 3500 rpm for 5

minutes. These centrifuge cycles were completed to purify AgNP. Extracellular Ag NPs (RAE-AgNPs) synthesis from RAE was completed. After the reaction, the biomass was separated by the centrifuge and stored at -20 °C until characterization.

To prepare the BAE extract, 3.0 g (wet weight) algal biomass was suspended in 20 ml deionized water and heated to 100 °C for 20 minutes in an erlenmeyer flask. After the boiling procedure, it was cooled and filtered with Grade GF/A glass microfiber filters (Whatman™, pore size: 1,6μm). The obtained filtrate had the final concentration of 5 mM AgNO$_3$ added at room temperature to begin the reaction. After the procedure continuous mixing was completed. Later the mixing procedure, a colloidal structure was obtained and after this process repeated centrifugation was completed at 3500 rpm for 5 minutes. These centrifuge cycles were completed to purify AgNP. Extracellular Ag NPs synthesis (BAE-AgNPs) from boiled algal extract was completed. After the reaction had completed, the biomass was separated by the centrifuge and stored at -20 °C until characterization.

Characterization of AgNPs

Biological reduction of silver ions with the green synthesis route was observed by taking 3 ml aliquot samples at different time intervals. Absorption measurements were made with a UV-Vis (AE-S90-2D UV-VIS Spectrophotometer, China.) spectrophotometer between 190 and 1100 nm.

Transmission electron microscope (TEM) images of the intracellular and extracellular synthesized AgNPs were obtained using TEM (JEOL JEM 1220 brand, Japan) working at 100 kV acceleration voltage. Samples used to obtain TEM micrographs were prepared by dropping on a carbon-coated copper grid and dried under a vacuum before investigation. With the aim of investigating the cells at the ultrastructural level, routine TEM monitoring procedure was performed and samples were submerged in epoxy resin. Thin sections were taken at 60 nm thickness with the aid of an ultramicrotome (Leica ultracut UCT, Leica, Germany) (Ilknur et al. 2012; Li et al. 2012; Zhang et al. 2016). Elemental analysis of samples was completed with SEM (a JEOL JSM-5600 LV brand, Japan) device fitted with EDS (E2V Scientific Instruments, United Kingdom).

Algae cells were freeze-dried and algae biomass was obtained. Dried biomass was prepared using the KBr pellet technique and ATR technique. The surface chemistry of reduced Ag samples and the biologically active portions of the live microalgal cells were analyzed to check for comparisons. The fourier transform mid-infra-

red FTIR spectra (Perkin Elmer Spectrum 100 FTIR-ATR unit, Germany) were collected with conduction mode from 400–4,000 cm^{-1} with 0,4 cm^{-1} spatial resolution.

Dynamic light scattering (DLS) and zeta potential are necessary parameters to define the size distribution, particle size, homogeneity and stability of LAC-AgNPs, RAE-AgNPs and BAE-AgNPs. Particle size and polydispersity index (PDI) were determined using the dynamic light scattering technique. DLS studies of LAC-AgNPs, RAE-AgNPs and BAE-AgNPs diluted in deionized water were measured by a Malvern-Zetasizer (Nano-Z590, United Kingdom) device. The zeta potential is a measurement of the attraction or repulsion values between particles. Particles with certain load attractions with opposite polarity within the suspension, as a result, a strong bond surface is formed on the surface of the loaded particle and then a surface extending outward from the loaded particle forms. The behavior of particles within polar fluids is determined not by electric load but by zeta values. Zeta potential studies were measured with a Malvern (SN: MAL1064144, United Kingdom) brand Zeta Sizer ZS device.

Antimicrobial Susceptibility Testing of synthesis NPs

In this study with the aim of determining the antibacterial and antifungal susceptibility of LAC-AgNPs, RAE-AgNPs and BAE-AgNPs, *Salmonella* sp. (gram-) and *Listeria monocytogenesis* (gram+) bacteria and *Candida parapsilosis* yeast was used. To determine the minimal inhibition concentration, the broth microdilution method was taken as a basis. Bacteria cells were left in nutrient broth medium at 37 °C for 1 night, while yeast cells were incubated for 1 night in a shaking incubator at 30 °C in yeast extract-peptone-dextrose (YPD; %1 yeast extract, %2 peptone %2 dextrose) medium and cultures were taken. The density of bacteria and fungal cells were set according to the McFarland 0.5 standard. Tests of minimal inhibitory concentration (MIC) were made in accordance with the CLSI (Clinical Laboratory Standards Institute) criteria M27-A8 for bacteria and M27-A2 for yeast (Zgoda and Porter 2001). The extraction containing lowest NPs that inhibited bacterial and fungal development was determined as the volume MIC value. During this process 40 minutes sonication was applied to obtain the LAC-AgNPs. The 96-well plates (Lp Italiana Spa) was added 100 μl RPMI 1640 and 100 μl the LAC-AgNPs, RAE-AgNPs and BAE-AgNPs. Later they were diluted with microdilution and left for 24 hours incubation. The plate with resazurin added had results assessed in parallel with the colour change.

RESULTS

The test organism *Desmodesmus* sp. (KR261937) is in the Chlorophyceae class and is a water alga generally forming colonies with an oval or shuttle-shaped body. Additionally, it is a photosynthetic microalga with 6-10 horn-like protrusions on the body. In the colonial structure, generally twin cells are found. Additionally, sequences of 4 colonial cells may be seen in low numbers. The count of the automatic cell counting device is given in Table 1. In the current study when algal biomass (LAC) was exposed to Ag ions (Ag$^+$), the colour of the algal biomass changed from natural bright green to brown and compared with the control biomass, the Ag$^+$ ion was biologically transformed (Ag metal accumulation) to Ag^0. During exposure the colour change began in the first 24 hours; however, the largest colour difference compared to the first day occurred after 72 hours. LAC-AgNPs was researched with UV-Vis for 72 hours (Figure 1A).

Simultaneously RAE and BAE were treated with 5 mM AgNO$_3$ and extracellular Ag NPs (RAE-AgNPs and BAE-AgNPs) the formation was researched with UV-Vis spectroscopy. The RAE-AgNPs were colourless and had a high peak at 280-300 nm (Figure 1 B). The RAE exposed to Ag displayed a peak at 420 nm especially after the 48 hours day on UV-Vis spectral analysis and it was considered AgNP formation had begun. It is known that the concentration of the reducing agent in the reaction mixture plays an important role in the formation of nucleation points and then controls the size of AgNP; this may have caused less stable AgNP in the RAE (Hiramutsu and Osterloh 2004; Jena et al. 2014).

As a result, another experiment was made to increase the concentration of this type of material in the reaction mixture. The biomass was boiled in water to obtain more reducing and stabilizing agents. Initially, the boiled extract had a light yellow colour, which transformed to brown when exposed to the Ag nitrate solution procedure. The formation of this colour is due to stimulation of surface plasmon resonance (SPR) effect and the reduction in AgNO$_3$ and may indicate the formation of AgNP. With the increase in the reaction duration, the colour of the reaction mixture turned a darker

Table 1. *Desmodesmus* sp. cell counting and cell viability analysis report.

Total cell	Live cell	Dead cell	Viability
4,48x10^8	4,08x10^8	4,00x10^7	80,6 %

*Stain: Trypan blue.
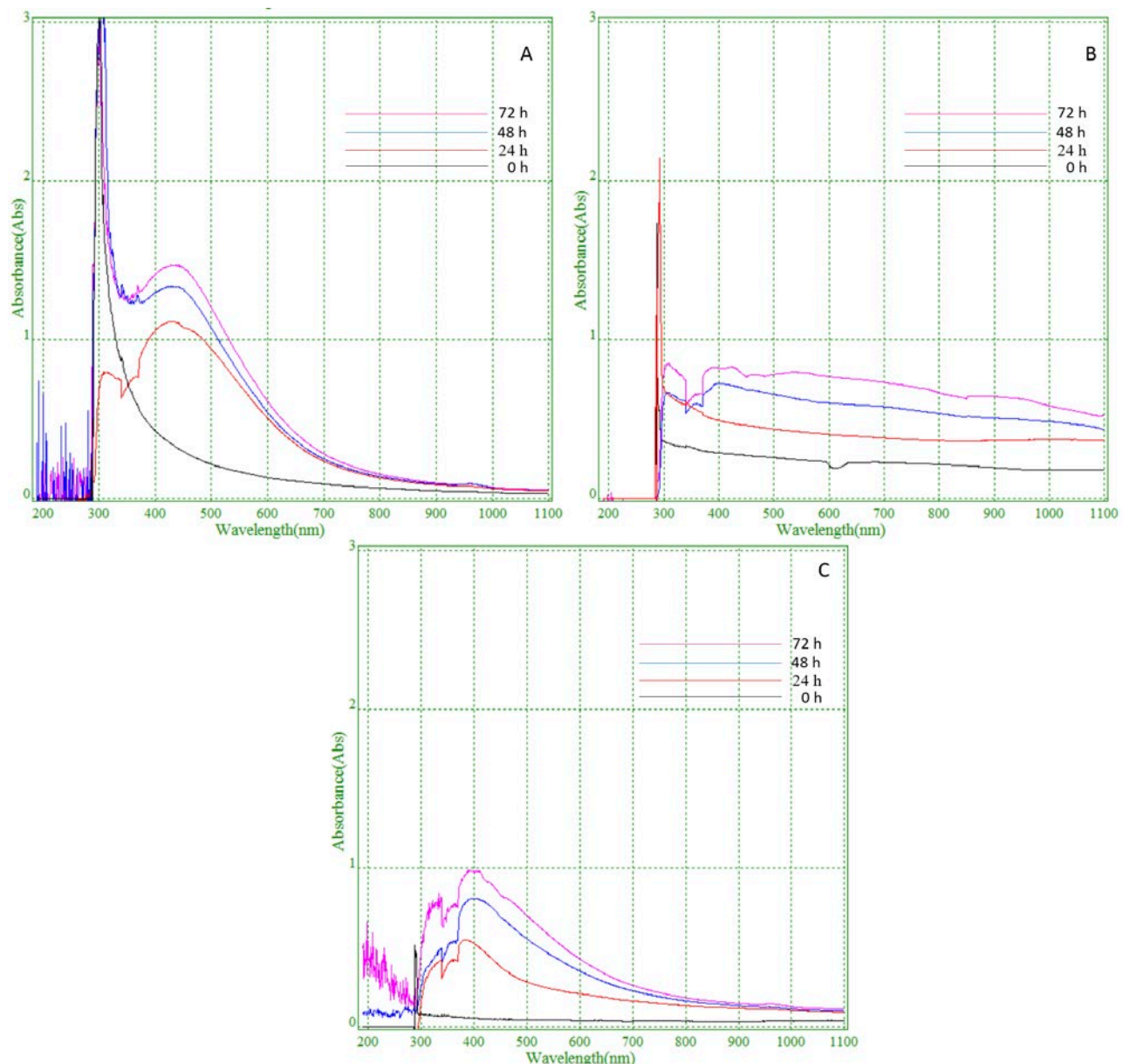
Fig. 1. Examination of intracellular and extracellular synthesis of silver nanoparticles by UV-Vis. A. LAC-AgNPs; B. RAE-AgNPs; C. BAE-AgNPs.

shade for up to 72 hours. The formation of BAE-AgNPs were proven with the UV-Vis spectrum showing the characteristic surface plasmon resonance (SPR) band for AgNPs. Figure 1 C shows the UV-Vis spectra series recorded for the reaction mixture at a variety of time intervals. The BAE showed a peak at 280-320 nm which may be linked to the presence of peptides. The BAE exposed to Ag displayed a peak at 420 nm especially after the 24 hours day on UV-Vis spectral analysis and it was considered BAE-AgNPs formation had begun.

Our UV-Vis results show a steady increase in reduction of Ag ions in LAC up to 420 nm, then it stabilized and appeared to pass to a downward trend. This section is defined as the "surface plasmon resonance band" and is due to the stimulation of free electrons in the NPs. The symmetric shape of the band is an indicator of the regular distribution of the spherical NPs (Travan et al. 2009).

After intracellular synthesis, the exposed biomass had TEM analysis was made to research the morphology
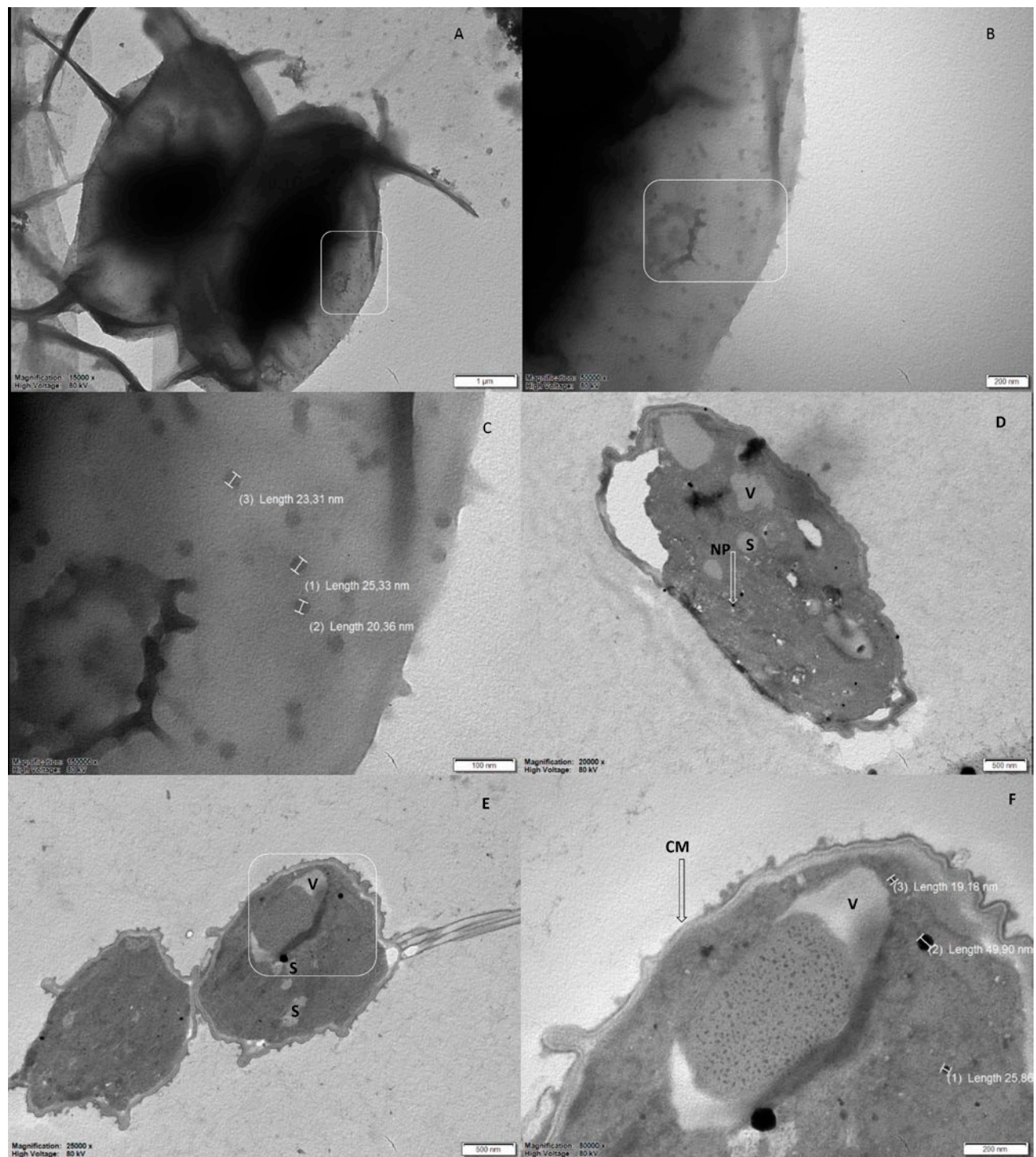
Fig. 2. Morphological characterization of the silver nanoparticles. A, B, C Intracellular synthesis, TEM Image of *Desmodesmus* sp. cell mediated synthesized silver nanoparticles. D, E, F Cellular localization of in Intracellular silver nanoparticles, TEM micrograph of thin section (~ 60 nm). NP:nanoparticle, S starch, V vakuol, CM Cytoplasmic membrane.

and dimensions of the NPs. TEM images revealed the cells were nearly 4.5-5 μm (length) × 2-3 μm (width) size with an oval shape and with 6-9 colonial protrusions (Figure 2A).
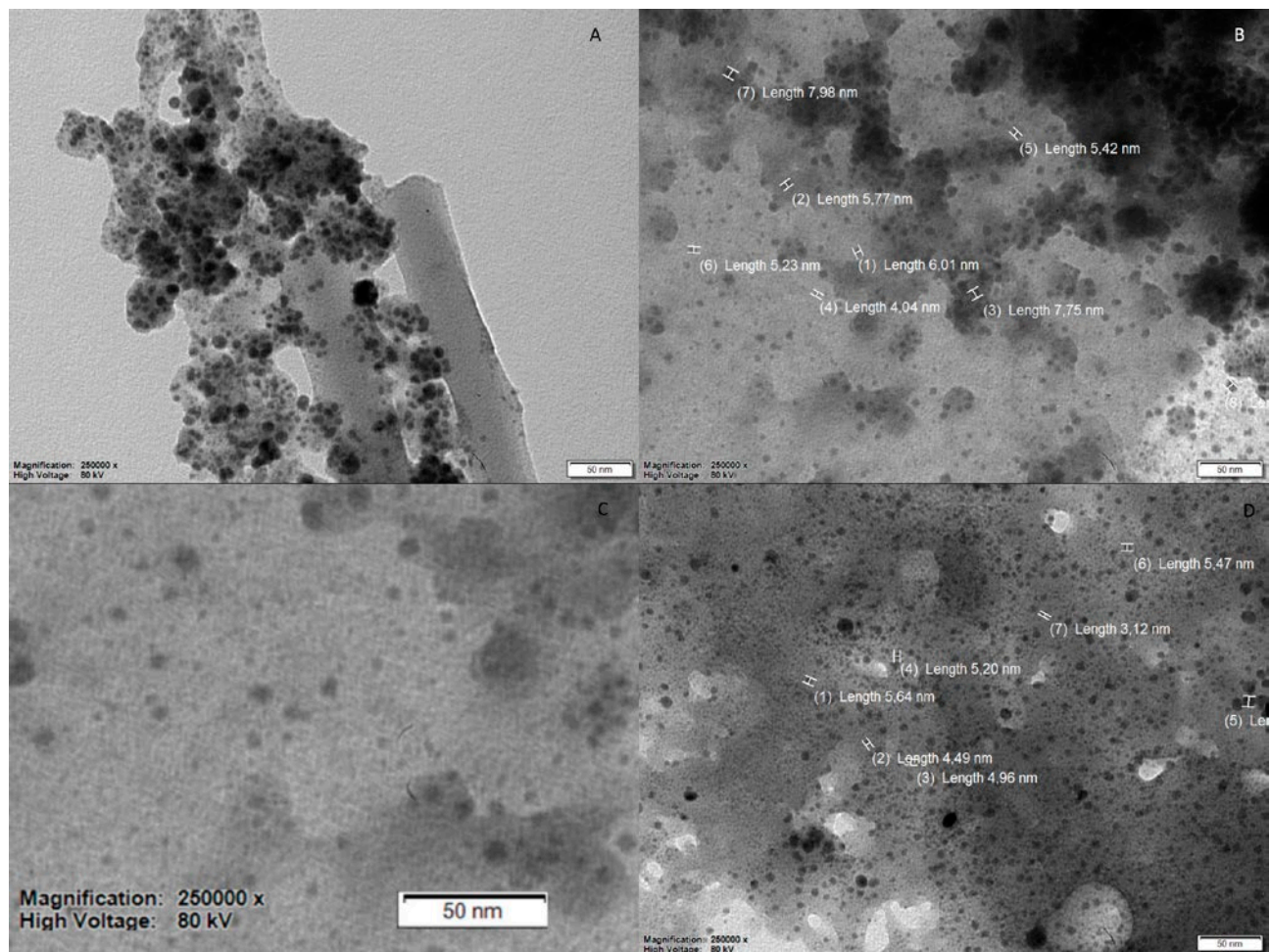
Fig. 3. TEM Image of extracellular synthesized silver nanoparticles A, B. *Desmodesmus* sp. cell RAE mediated synthesized silver nanoparticles (RAE-AgNPs); C, D. *Desmodesmus* sp. cell BAE mediated synthesized silver nanoparticles (BAE-AgNPs).

When the algae cells exposed to $AgNO_3$ were investigated with TEM on a grid with the dropping method, distributed metal NPs were observed, as shown in Figure 2 A, B and C. As seen at different magnifications of the metal nanoparticle shapes, the periphery of the cells is observed more clearly and homogeneously, while the interior sections were not fully identified due to a more compact and electron-dense zone observed (Figure 2 A, B). When micrographs of LAC-AgNPs at high magnifications are investigated, the spherical structures of the AgNPs are clearly observed. The intracellular LAC-AgNPs are in the range of 10-30 nm in size and appear to display a homogeneous distribution. In TEM analysis, a section of 60 nm in thickness was taken from the cells in order to be able to see the LAC-AgNPs. Additionally, sections were taken of these cells to identify where the NPs were localized (Figure 2 D, E, F). According to the results of these sections, NPs were localized especially in areas close to the cell membrane, while also in other regions of the cell, e.g., in areas close to starch storage areas (Figure 2 F).

The nanoparticle dimensions obtained after RAE-AgNPs were mean 4-8 nm (Figure 3 A, B). NPs synthesized in this manner were less stable according to both TEM and zeta potential results. When morphology and size of NPs are examined after extracellular synthesis, the NPs produced by BAE-AgNPs were mean 3-6 nm. These NPs had a homogeneous distribution without aggregation or flocculation (Figure 3 C, D). The reason for this is that some stabilizing agents in the algal extract were released by boiling and entered the reaction (Mohseniazar et al. 2011; Nithya and Ragunathan, 2009). At the same time, control of dimension and structure may be associated with interactions between biocomponents like polysaccharides, proteins, polyphenols and phenolic compounds with metal atoms (Shao et

Table 2. EDS reported from biosynthesized AgNPs.

AgNPs	Intensity (c/s)	Error 2-sig	Conc.	Units
Control	0.060	0.129	0.023	wt.%
LAC-AgNPs	130.34	7.217	34.385	wt.%
RAE- AgNPs	130.01	7.209	20.975	wt.%
BAE- AgNPs	293.68	10.837	54.920	wt.%

*kV 20.0, Takeoff Angle 35.0°.
Elapsed Livetime 10.0.
Conc: Concentration.

al. 2004). As a result, BAE-AgNPs showed the NPs had equal distribution.

Analysis through Energy dispersive SEM-EDS spectrometers confirmed the presence of an elemental Ag signal of the Ag NPs. Recognition lines for the major emission energies for Ag are displayed and these match with peaks in the spectrum, thus giving confidence that Ag has been correctly identified. In this study, the synthesized AgNPs were subjected to elemental analysis with SEM-EDS, the Ag element was observed in all three situations (LAC-AgNPs, BAE-AgNPs, RAE-AgNPs) at the rate (Table 2) (Figure 4 A, B, C). The highest Ag was identified in the BAE-AgNPs groups (Figure 4 B). When these results are considered, they provide information about the purity of the formed NPs.

Extracts obtained with different methods (BAE and RAE) and live cell algae (LAC) the AgNPs obtained from these extracts (LAC-AgNPs, RAE-AgNPs and BAE-AgNPs) had FTIR analysis completed on these samples to define the functional groups of chemical components. The analysis results observed many peaks (transmittance a.u) at 3284, 2919, 2851, 2161, 2027, 2034, 1638, 1535, 1380, 1242, 1149, 1023, 812, 717, and 551.

When vibrations of biomass exposed to Ag are investigated, the dense broadband at 3400 cm^{-1} is vibrations from alcoholic, phenolic and carboxylic groups (Figure 1 F). Primarily in addition to hydroxyl groups equivalent to O-H strain, vibrations equivalent to primary and secondary amines and amides are shown with N-H strain were observed. The band at nearly 2920 cm^{-1} reflects the C-H strain of alkanes. The lack of absorption in this region shows hydrogen linked to aliphatic carbon is not present (Rónavári et al. 2017). The band at 2851 cm^{-1} from the aldehyde group reflects C-H strain. The band at 2161 cm^{-1} is -S-C≡N thiocyanate, while the bands at 2027 and 2034 cm^{-1} are -N=C=S isothiocyanate. This situation shows that cyanate, elemental carbon and thiocyanate may be found within total organic carbon. The peak at nearly 1,638 cm^{-1} is equivalent to C = C vibration of aromatic structures, with the peak at 1242 cm^{-1} equivalent to C-O strain of phenolic groups. The peak at 1380 cm^{-1} is NO$_2$ asymmetric strain of
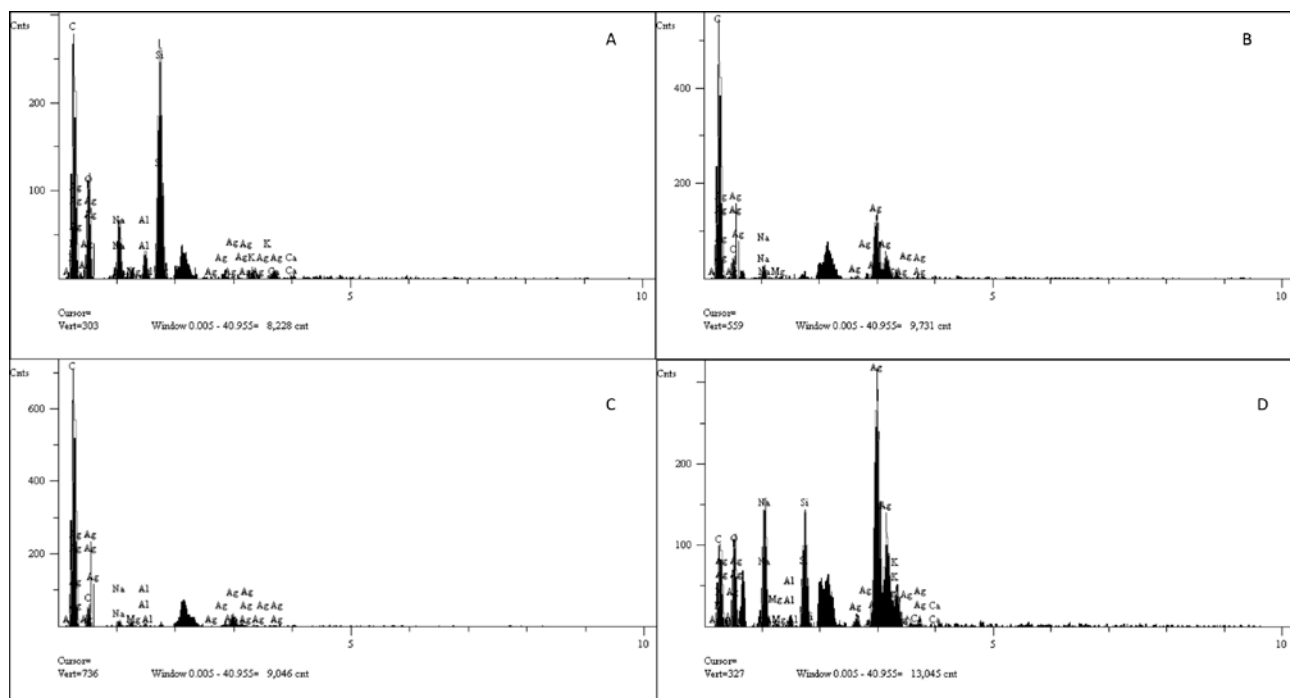
Fig. 4. SEM-EDS spectrum recorded from biosynthesized AgNPs A. Control group; B. LAC-AgNPs; C. RAE-AgNPs; D. BAE-AgNPs.
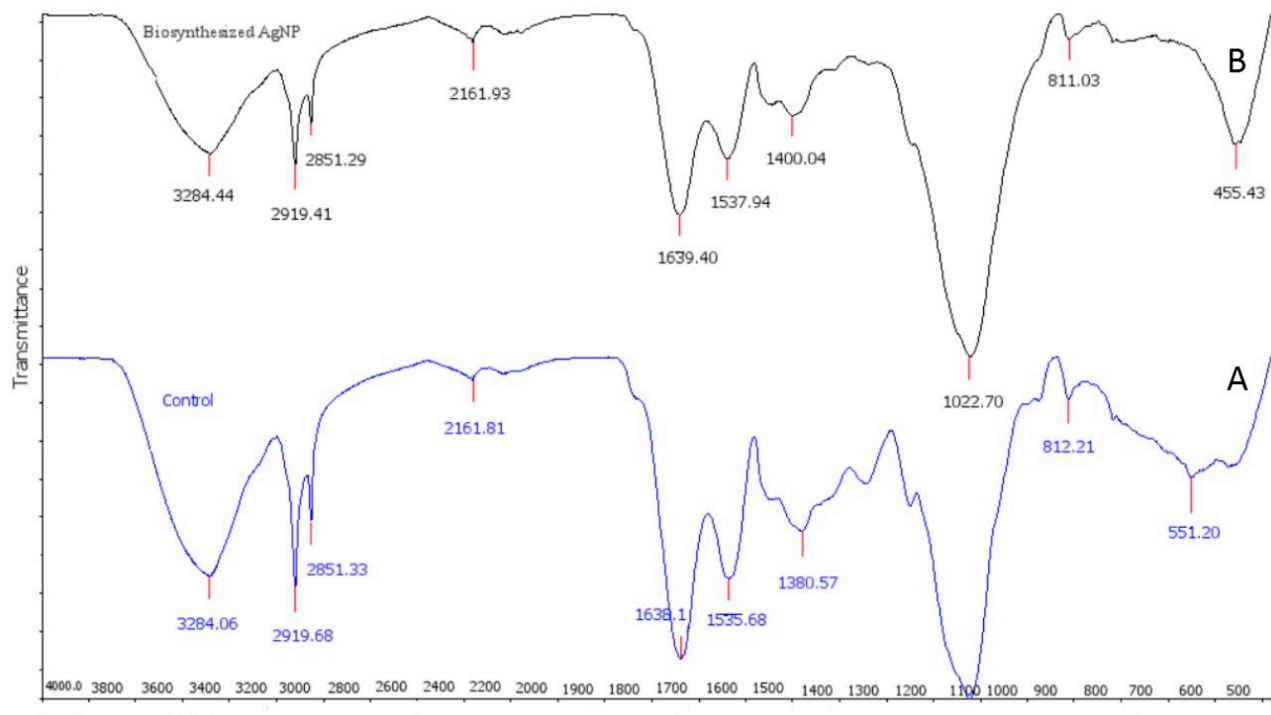
Fig. 5. FT-IR spectrum for A. *Desmodesmus* sp. control group; B. *Desmodesmus* sp. formed LAC-AgNPs.

alkyl groups, and the peak at 1535 cm^{-1} is equivalent to C = C strain of biphenol group. Around 1145 cm^{-1} the C-N strain vibration of aromatic primary and secondary amines is observed. Aromacity may be mentioned between 900-690 cm^{-1} (Jena et al. 2014).

The extracellular BAE-AgNPs obtained with the boiling method may have bonded to amine groups, while the RAE-AgNPs may have bonded to alkyne groups. Our FTIR results comply well with the literature data, with the surface of AgNPs obtained from intracellular *Desmodesmus* sp. coated with organic components found in the extract, as shown in Figure 3 B. As a result, successful green synthesis is revealed with the soluble organic components or proteins able to bind to Ag ions and reduce Ag ions to form NPs (Jegadeeswaran et al. 2012) (see 800-2919 cm^{-1} region).

Particle size and zeta potential are very important parameters for green synthesized Ag NPs. The particle size of Ag NPs, especially, has a large effect on the antimicrobial properties. Another important value for particle size is PDI. PDI reveals homogeneity (Sharma et al. 2018). Both intracellular and extracellular AgNPs were well distributed in colloidal solution and the mean size distribution of these particles were as follows; the mean particle distribution for LAC-AgNPs were 10-30 nm, with this value 4-8 nm and 3-6 nm from RAE-AgNPs and BAE-AgNPs (Figure 6 A, C, E). According to PDI

values for the results, homogeneous particle size distribution within the solution was observed to be highest for LAC-AgNPs. Though different sizes were found during synthesis, higher numbers of small-scale NPs were observed in terms of numbers (Table 3).

Zeta potential values are obtained from the high repulsion and attraction forces between each nanoparticle and these values define particle stability. Intracellular and extracellular AgNPs have high negative zeta potential values. The high negative value affects the push between the particles, thereby increasing the stability of the formulation (Rao et al. 2013). In our study, the zeta potential of AgNPs were measured as -20.2 mV for LAC-AgNPs (Figure 6 B), -19.9 mV for BAE-AgNPs (Figure 6 D) and -14.2 mV for RAE-AgNPs (Figure 6 F). All values for particle sizes, PDI and zeta potentials are shown in

Table 3. The particle size of silver nanoparticles, polydispersity index and Zeta potential.

	Particle size (nm) DLS	PDI	Zeta potential (mV)
LAC-AgNPs	20-40	0.445	-20.2
BAE-AgNPs	10-15	0.452	-19.9
RAE-AgNPs	10-20	0.613	-14.2
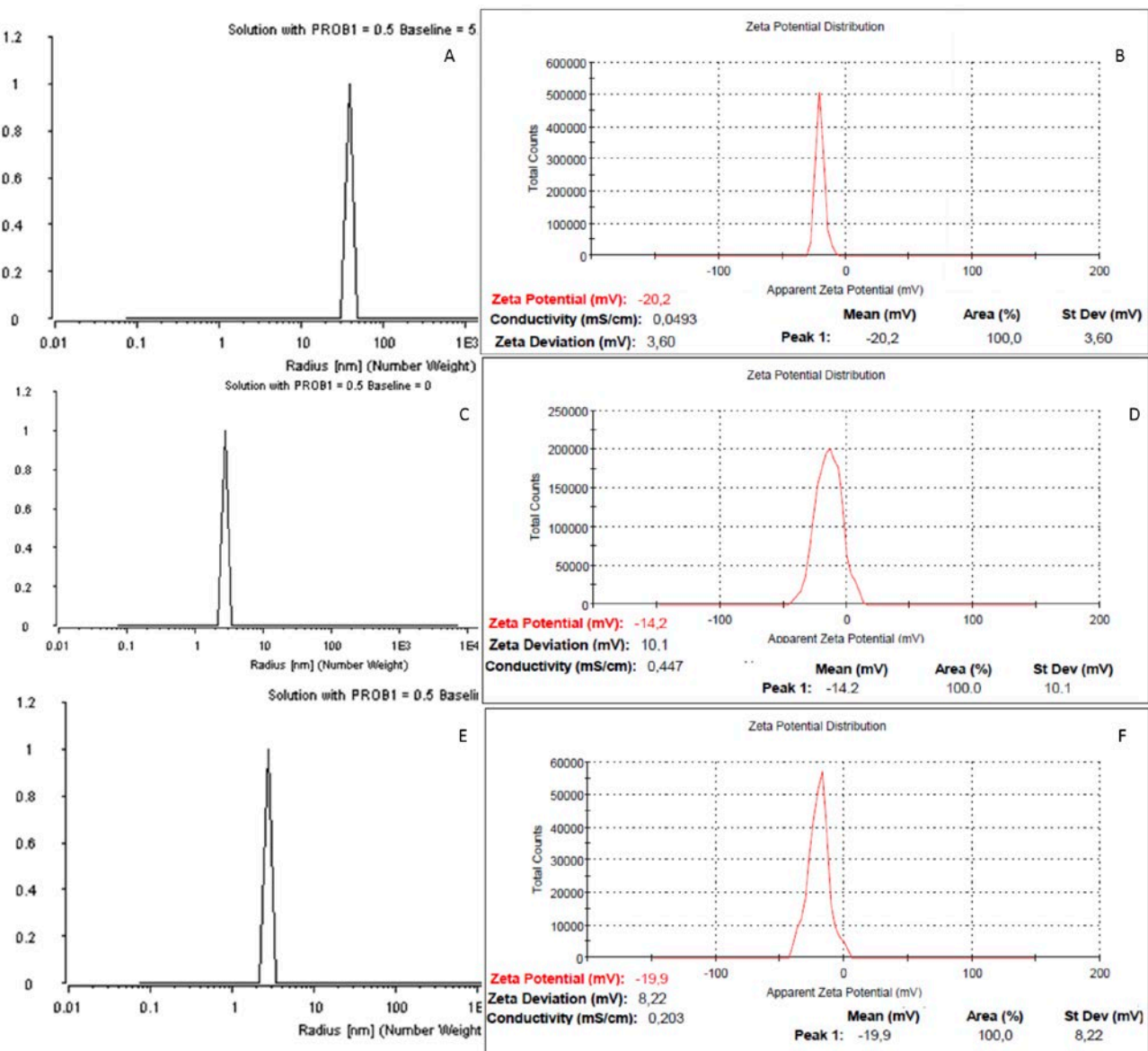
Fig. 6. Size distribution by dynamic light scattering and zeta potential measurement of biyosenthesis silver nanoparticles A, B. LAC-AgNPs; C, D. RAE-AgNPs; E, F. BAE-AgNPs.

Table 3. The observed result contains some differences compared with the TEM studies but is well-correlated. The differences may be due to the tendency of Ag NPs to agglomerate within an aqueous solution; thus the values obtained from DLS will be higher than TEM values (Domingos et al. 2009).

Antimicrobial and antifungal effect of synthesis AgNPs

LAC-AgNPs, RAE-AgNPs and BAE-AgNPs have been tested on *Salmonella* sp. (gram +) and *Listeria monocytogenesis* (gram -), the most frequently encountered bacteria in food poisoning (Cantero et al. 2018; Ma et al. 2018). The MIC values of the synthesized NPs were calculated on these bacteria. It was initiated by adding 100 µl of synthesized NPs so that the MIC values could be found. The LAC-AgNPs, RAE-AgNPs and BAE-AgNPs inhibited 3,125 µl of *Salmonella* sp. Thus, this value was determined as the MIC value. There was a larger effect on *Listeria monocytogenesis* compared to *Salmonella* sp. with 1,5625 µl MIC value determined. *Candida parapsilosis* is a pathogenic yeast strain with

Intracellular and extracellular green synthesis of silver nanoparticles using *Desmodesmus* sp.

39

high biofilm formation capacity (Soldini et al. 2017). *Candida parapsilosis* appeared to be more affected compared to bacteria and the MIC value was determined as 0,78125 μl (The synthesized AgNPs were initially used in 100 μl). The LAC-AgNPs, BAE-AgNPs and RAE-AgNPs obtained from *Desmodesmus* sp. with different methods showed significant degree of effect with different MIC values for bacteria and yeast.

DISCUSSION

AgNP is used in a variety of applications like catalysis, biosensing, imaging and antibacterial activity. As result researchers in recent times have performed many studies to synthesize AgNP more economically and easily. Green synthesis is an alternative method developed to produce metal NPs using natural compounds or plant components. The most important advantages of these methods are the lack of toxic material involved in the chemical synthesis and the lack of high costs. In addition to green synthesis and sustainable synthetic methods can decrease environmental pollution to some extent (Khatami et al. 2018c) . Another significant advantage is that NPs may be synthesized in an easy and reliable manner using only live organisms (algae, bacteria, fungus and plant), without requiring reducing or stabilizing agents (Tippayawat et al. 2016; Khatami et al. 2018b). Microorganisms such as bacteria and algae have proven to be well suited for nanoparticle synthesis, where particle size and morphology must be stabilized by different methods in green synthesis (Metuku et al. 2014). Algae or plants or their extracts, many prokaryotic organisms and biocompatible macromolecules are very important for nanoparticle synthesis (Poulose et al. 2014). Algae are unique due to the lipids, minerals and some vitamin wealth contained in these organisms (Namvar et al. 2012; Zuercher et al. 2006). Additionally, polysaccharides, proteins, and polyphenols are known as functional food as a variety of bioactive material with some medical uses like in cancer, oxidative stress, inflammation, allergies, thrombosis and lipidemia (Mahdavi et al. 2013). As a result, hydroxyl, carboxyl and amino functional groups are found among this phytochemical material that is capable of acting in a single step as both effective metals reducing agents and as capping agents. Generally many natural essences in cell contents or released after extraction are biologically active compounds and may be responsible for the reduction of Ag ions and stabilization of the obtained NPs.

The carbonyl groups in proteins have strong binding ability against metal NPs and as a result, proteins may form a coating layer on the surface of AgNPs (Dhand et al, 2016; Vivek et al. 2012). This may prevent agglomeration and increase the stability of NPs synthesized in aqueous media. In our study, UV-Vis data from algal cells exposed to Ag nitrate support the view that of Ag $^+$ ions were taken into cells within 24 hours and L-AgNPs formed (Peaked at 420 nm within 24 h.). As metal ions (Ag$^+$) are on the algal surface, they were identified to be held by electrostatic interaction between the functional groups with the negative load on the cell surface, and following this, the metal ions were reduced (Barwal et al. 2011). In this way, high intracellular accumulation and formation of metal particles may be linked to several probable mechanisms in the process. These mechanisms vary according to type and metal accumulation occurs with two processes. The first is adsorption or biosorption at the cell surface independent of metabolism, while the second is metabolism-dependent absorption by organelles or cytoplasmic ligands (Chakraborty et al. 2006).

Metal NPs synthesized with green methods may produce colloids with different sizes, shapes, and distributions. If changing the method used provides better results, the green approach may be chosen. As a result of our study, the focus was on the biosynthesis of both intracellular and extracellular AgNP using different extraction techniques with *Desmodesmus* sp. microalgae and AgNP production was successfully achieved. In this study during intracellular synthesis, algal cells have pores of 3-5 nm width ensuring passage of low molecular weight material like water, inorganic ions, gases and other small nutritional material required for growth and metabolism (Wang and Chen 2009). Large molecules or macromolecules cannot pass these pores. Similarly, in our study, the intracellular LAC-AgNPs appeared to be larger than the size of the pores in the algal cell walls (10-30 nm) (Figure 2 A, B, C). The BAE-AgNPs and RAE-AgNPs also had spherical shape without agglomeration. Sections through the cells transversely and longitudinally observed nanoparticle formation distributed through intracellular cytoplasm, with larger size NPs in some regions, e.g., in regions close to vacuoles. In previous research, it was reported that maximum metal accumulation occurred within the cytoplasm, periplasm, nucleus and pyrenoids of organisms like *Chlamydomonas* (Ag), *Chlorella* (Au, Pd, Ru, Rh), *Klebsormidium flaccidum* (Au) and *Shewanella* (Au, Pt) (Barwal et al. 2011; Dahoumane et al. 2012; Luangpipat et al. 2011).

FTIR can be used to identify the type of functional groups and biomolecules that are responsible for capping and efficient stabilization of NPs and qualitative and quantitative identification of the molecular structure

of organic compounds in the NPs structure (Khatami et al. 2018d). In thi study, the results of FTIR spectroscopic investigations showed the presence of organic particles especially in the 800-2919 cm⁻¹ region. Linked to this result, the protein building block of amino acids was confirmed as having strong binding ability to metals and formed a layer surrounding metal NPs. They acted as a coating material preventing agglomeration and thus are considered to have ensured high stability of metal NPs. These results confirm the presence of proteins or peptides with possible function as stabilizing agents for AgNPs (Singhal et al. 2011).

The extracellular RAE-AgNPs synthesized was found to be less stable and have a tendency to agglomerate compared to extracellular synthesized BAE-AgNPs and intracellular synthesized L-AgNPs. Additionally, the RAE-AgNPs synthesis process was slower compared to the others. When BAE was used, both high rates of BAE-AgNPs biosynthesis occurred and the stability of these NPs were higher. However, according to the UV results, L-AgNPs were more rapid biosynthesised than extracellular BAE-AgNPs and RAE-AgNPs. This situation may be related to macromolecules like protein or peptide released by boiling directly reducing Ag⁺ ions. A study by Jena et al. (2014) produced similar results. The researchers explained that in this situation the protein or peptide concentration has a vital role in AgNP formation and stabilization. A similar study by Barwal et al. (2011) prepared *Chlamydomonas* cell extract treated with Ag nitrate with both whole cell esence and protein-removed extraction. When the results are compared, the protein-removed cell extraction was identified to synthesize larger sizes of AgNP. The researchers explained that the protein concentration is directly correlated with particle formation rate and inversely correlated with particle size (Barwal et al. 2011; Jena et al. 2014).

Due to a variety of reasons in the antimicrobial mechanism, Ag ions or salts only have limited use as an antimicrobial agent. However, the use of AgNPs may overcome these limitations. In biological systems (animal cell culture, plants, bacteria) the effect of AgNPs in different concentrations has been investigated (Sobieh et al. 2016, Khatami et al. 2018). For the use of Ag against microorganisms in a variety of areas, it is important to prepare Ag with appropriately priced methods and to know the antimicrobial effect mechanism to increase this effect (Kim et al. 2007). Green synthesized NPs may expand these areas of use significantly. In this study, AgNPs may be a potential antibacterial and antifungal agent and could be prepared cost-effectively. Because, *Desmodesmus* sp., a green algae, could be a low-cost production house for intracellular and extracellular AgNPs

synthesis because of the minimum growth regimens required for growth, such as water, sunlight and commercial fertilizers, and high biomass efficiency.

CONCLUSION

In this study different sizes of AgNP were successfully synthesized from *Desmodesmus* sp. microalgae using both intracellular and extracellular green synthesis routes. In particular, intracellular UV results of LAC-AgNPs peaked at 420 nm within the first 24 hours. The purity of Ag NPs was confirmed with SEM-EDS. Nanoparticle size and stability were determined according to DLS and Zeta potential results. AgNPs with optimized size were determined to have lethal potential against bacteria and yeast. Thus this study is considered to support sustainable development of green synthesis using the green microalgae of *Desmodesmus* sp.

REFERENCES

Annamalai J and Nallamuthu T. 2015. Characterization of biosynthesized gold nanoparticles from aqueous extract of *Chlorella vulgaris* and their anti-pathogenic properties. Applied Nanoscience, 5(5), 603-607. DOI 10.1007/s13204-014-0353-y

Barwal I, Ranjan P, Kateriya S, Yadav SC. 2011. Cellular oxido-reductive proteins of *Chlamydomonas reinhardtii* control the biosynthesis of silver nanoparticles. Journal of nanobiotechnology, 9(1), 56. DOI 10.1186/1477-3155-9-56

Boroumand Moghaddam A, Namvar F, Moniri M, Md Tahir P, Azizi S, Mohamad R. 2015. Nanoparticles biosynthesized by fungi and yeast: a review of their preparation, properties, and medical applications. Molecules, 20(9), 16540-16565. DOI 10.3390/molecules200916540

Cantero G, Correa-Fiz F, Ronco T, Strube M, Cerdà-Cuéllar M, Pedersen K. 2018. Characterization of Campylobacter jejuni and Campylobacter coli Broiler

Isolates by Whole-Genome Sequencing. Foodborne pathogens and disease, 15(3), 145-152. DOI 10.1089/fpd.2017.2325

Chakraborty N, Pal R, Ramaswami A, Nayak D, Lahiri S. 2006. Diatom: a potential bio-accumulator of gold. Journal of radioanalytical and nuclear chemistry, 270(3), 645-649. DOI 10.1007/s10967-006-0475-0

Dağlıoğlu Y, Çelebi SM, Önalan Ş. 2016. Determination of acute toxic effects of poly (Vinylferrocenium) supported palladium nanoparticle (Pd/PVF+) on *Artemia salina*. Pakistan Journal of Zoology, 48(1), 187–193.

Dağlıoğlu Y, Kabakcı D, Akdeniz G, Çelebi MS. 2016. Determining the acute toxic effects of poly(vinylferrocenium) supported platinum nanoparticle (PT/PVF+ NPs) on *Apis mellifera*.

Dağlıoğlu Y, Öztürk BY. 2016. The assessment of biological accumulation on exposure in boron particles of *Desmodesmus multivariabilis*. Biological Diversity and Conservation. 9(3), 204-209.

Dağlıoğlu Y, Öztürk BY. 2018. Effect of concentration and exposure time of ZnO-TiO$_2$ nanocomposite on photosynthetic pigment contents, ROS production ability, and bioaccumulation of freshwater algae (*Desmodesmus multivariabilis*). Caryologia, 71(1), 13-23, DOI 10.1080/00087114.2017.1400262

Dağlıoğlu Y, Türkiş S. 2017. Effect of nano and microparticle boron on hydrogen peroxide (H$_2$O$_2$) and lipid peroxidation (MDA) enzyme activity superoxide dismutase (SOD) of *Myriophyllum spicatum*. 6(2), 62-70.

Dağlıoğlu Y, Türkiş S. 2017. Effect of TiO$_2$ nanoparticles application on photosynthetic pigment contents of duckweed (*Lemna minor* L.). Acta Biologica Turcica, 30(4), 108-115.

Dahoumane SA, Djediat C, Yéprémian C, Couté A, Fiévet F, Coradin T, Brayner R. 2012. Recycling and adaptation of Klebsormidium flaccidum microalgae for the sustained production of gold nanoparticles. Biotechnology and bioengineering, 109(1), 284-288. DOI doi.org/10.1002/bit.23276

Dhand V, Soumya L, Bharadwaj S, Chakra S, Bhatt D, Sreedhar B. 2016. Green synthesis of silver nanoparticles using Coffea arabica seed extract and its antibacterial activity. Materials Science and Engineering: C, 58, 36-43. DOI 10.1016/j.msec.2015.08.018

Domingos RF, Baalousha MA, Ju-Nam Y, Reid MM, Tufenkji N, Lead JR, Wilkinson, KJ. 2009. Characterizing manufactured nanoparticles in the environment: multimethod determination of particle sizes. Environmental science & technology, 43(19), 7277-7284. DOI 10.1021/es900249m

Faulkner DJ. 2000. Marine natural products. Natural Product Reports, 17(1), 7-55.

Ge L, Li Q, Wang M, Ouyang J, Li X, Xing MM. 2014. Nanosilver particles in medical applications: synthesis, performance, and toxicity. International journal of nanomedicine, 9, 2399. DOI 10.2147/IJN.S55015

Govindaraju K, Kiruthiga V, Kumar VG, Singaravelu G. 2009. Extracellular synthesis of silver nanoparticles by a marine alga, *Sargassum wightii* Grevilli and their antibacterial effects. Journal of Nanoscience and Nanotechnology, 9(9), 5497-5501. DOI 10.1166/jnn.2009.1199

Hiramatsu H, Osterloh FE. 2004. A simple large-scale synthesis of nearly monodisperse gold and silver nanoparticles with adjustable sizes and with exchangeable surfactants. Chemistry of Materials, 16(13), 2509-2511. DOI 10.1021/cm049532v

Ilknur D, Yasemin O, Nuri K. 2012. Effect of disinfectants on biofilm development by five species of Candida. African Journal of Microbiology Research, 6(10), 2380-2386. DOI 10.5897/AJMR11.1427

Jegadeeswaran P, Shivaraj R, Venckatesh R. 2012. Green synthesis of silver nanoparticles from extract of *Padina tetrastromatica* leaf. Digest Journal of Nanomaterials and Biostructures, 7(3), 991-998.

Jena J, Pradhan N, Nayak RR, Dash BP, Sukla LB, Panda PK, Mishra BK. 2014. Microalga *Scenedesmus* sp.: a potential low-cost green machine for silver nanoparticle synthesis. Journal of Microbiology and Biotechnology, 24(4), 522-533. DOI 10.4014/jmb.1306.06014

Joerger R, Klaus T, Granqvist CG. 2000. Biologically Produced Silver–Carbon Composite Materials for Optically Functional Thin-Film Coatings. Advanced Materials, 12(6), 407-409. DOI 10.1002/(SICI)1521-4095(200003)12:6<407::AID-ADMA407>3.0.CO;2-O

Kannan RRR, Arumugam R, Ramya D, Manivannan K, Anantharaman P. 2013. Green synthesis of silver nanoparticles using marine macroalga *Chaetomorpha linum*. Applied Nanoscience, 3(3), 229-233. DOI 10.1007/s13204-012-0125-5

Khatami M, Alijani HQ, Heli H, Sharifi I. 2018a. Rectangular shaped zinc oxide nanoparticles: Green synthesis by Stevia and its biomedical efficiency. Ceramics International. DOI 10.1016/j.ceramint.2018.05.224

Khatami M, Sharifi I, Nobre MA, Zafarnia N, Aflatoonian MR. 2018b. Waste-grass-mediated green synthesis of silver nanoparticles and evaluation of their anticancer, antifungal and antibacterial activity. Green Chemistry Letters and Reviews, 11(2), 125-134. DOI 10.1080/17518253.2018.1444797

Khatami M, Alijani HQ, Nejad MS, Varma RS. 2018c. Core@ shell nanoparticles: greener synthesis using

natural plant products. Applied Sciences, 8(3), 411. DOI 10.3390/app8030411

Khatami M, Alijani H, Sharifi I. 2018d. Biosynthesis of bimetallic and core shell nanoparticles: their biomedical applications: A review. IET Nanobio, 1-19. DOI 10.1049/iet-nbt.2017.0308

Khatami M, Varma RS, Zafarnia N, Yaghoobi H, Sarani M, Kumar VG. 2018. Applications of green synthesized Ag, ZnO and Ag/ZnO nanoparticles for making clinical antimicrobial wound-healing bandages. Sustainable Chemistry and Pharmacy, 10, 9-15. DOI 10.1016/j.scp.2018.08.001

Kim JS, Kuk E, Yu KN, Kim JH, Park SJ, Lee HJ, Jeong, DHo, Hwang CY. 2007. Antimicrobial effects of silver nanoparticles. Nanomedicine: Nanotechnology, Biology and Medicine, 3(1), 95-101. DOI 10.1016/j.nano.2006.12.001

Kothari R, Pandey A, Ahmad S, Kumar A, Pathak VV, Tyagi V. 2017. Microalgal cultivation for value-added products: a critical enviro-economical assessment. 3 Biotech, 7(4), 243. DOI10.1007/s13205-017-0812-8

Kozma G, Rónavári A, Kónya Z, Kukovecz A. 2015. Environmentally benign synthesis methods of zerovalent iron nanoparticles. ACS Sustainable Chemistry & Engineering, 4(1), 291-297. DOI 10.1021/acssuschemeng.5b01185

Li L, Shi C, Yin Z, Jia R, Peng L, Kang S, Li Z. 2014. Antibacterial activity of α-terpineol may induce morphostructural alterations in *Escherichia coli*. Brazilian Journal of Microbiology, 45(4), 1409-1413. DOI 10.1590/S1517-83822014000400035

Luangpipat T, Beattie IR, Chisti Y, Haverkamp RG. 2011. Gold nanoparticles produced in a microalga. Journal of Nanoparticle Research, 13(12), 6439-6445. DOI doi.org/10.1007/s11051-011-0397-9

Ma X, Xu X, Xia Y, Wang Z. 2018. SERS aptasensor for *Salmonella typhimurium* detection based on spiny gold nanoparticles. Food Control, 84, 232-237. DOI 10.1016/j.foodcont.2017.07.016

Mahdavi M, Namvar F, Ahmad MB, Mohamad R. 2013. Green biosynthesis and characterization of magnetic iron oxide (Fe3O4) nanoparticles using seaweed (*Sargassum muticum*) aqueous extract. Molecules, 18(5), 5954-5964. DOI 10.3390/molecules18055954

Metuku RP, Pabba S, Burra S, Gudikandula K, Charya MS. 2014. Biosynthesis of silver nanoparticles from *Schizophyllum radiatum* HE 863742.1: their characterization and antimicrobial activity. 3 Biotech, 4(3), 227-234. DOI 10.1007/s13205-013-0138-0

Mohseniazar M, Barin M, Zarredar H, Alizadeh S, Shanehbandi D. 2011. Potential of microalgae and Lactobacilli in biosynthesis of silver nanoparticles. BioImpacts: BI, 1(3), 149. DOI 10.5681/bi.2011.020

Namvar F, Mohamed S, Fard SG, Behravan J, Mustapha NM, Alitheen NBM, Othman F. 2012. Polyphenolrich seaweed (*Eucheuma cottonii*) extract suppresses breast tumour via hormone modulation and apoptosis induction. Food chemistry, 130(2), 376-382. DOI 10.1016/j.foodchem.2011.07.054

Nithya R, Ragunathan R. 2009. Synthesis of silver nanoparticle using Pleurotus sajor caju and its antimicrobial study. Digest Journal of Nanomaterials and Biostructures, 4(4), 623-629.

Özkan Y, İrende İ, Akdeniz G, Kabakçı D, Sökmen M. 2015. Evaluation of the comparative acute toxic effects of TiO$_2$, Ag-TiO$_2$ and ZnO-TiO$_2$ composite nanoparticles on *Apis mellifera* (Honey Bee). J. Int. Environmental Application & Science, 10 (1), 26–36.

Öztürk BY, Dağlıoğlu Y. 2018. ZnO-TiO2 nanocomposite in *Chodatodesmus mucranulatus*. Fresenius Environmental Bulletin, 27(5), 2951-2962.

Poulose S, Panda T, Nair PP, Theodore T. 2014. Biosynthesis of silver nanoparticles. Journal of Nanoscience and Nanotechnology, 14(2), 2038-2049. DOI 10.1166/jnn.2014.9019

Pradeep T. 2009. Noble metal nanoparticles for water purification: a critical review. Thin solid films, 517(24), 6441-6478. DOI 10.1016/j.tsf.2009.03.195

Prasad TN, Kambala VSR, Naidu R. 2013. Phyconanotechnology: synthesis of silver nanoparticles using brown marine algae Cystophora moniliformis and their characterisation. Journal of applied phycology, 25(1), 177-182. DOI 10.1007/s10811-012-9851-z

Rajeshkumar S, Malarkodi C, Paulkumar K, Vanaja M, Gnanajobitha G, Annadurai G. 2014. Algae mediated green fabrication of silver nanoparticles and examination of its antifungal activity against clinical pathogens. International Journal of Metals, 2014. DOI 10.1155/2014/692643

Rao YS, Kotakadi VS, Prasad T, Reddy A, Gopal DS. 2013. Green synthesis and spectral characterization of silver nanoparticles from Lakshmi tulasi (*Ocimum sanctum*) leaf extract. Spectrochimica Acta Part A: Molecular and Biomolecular Spectroscopy, 103, 156-159. DOI 10.1016/j.saa.2012.11.028

Rippka R. 1988. [1] Isolation and purification of cyanobacteria. In Methods in Enzymology, Academic Press, 167, 3-27. DOI 10.1016/0076-6879(88)67004-2

Rónavári A, Kovács D, Igaz N, Vágvölgyi C, Boros IM, Kónya Z, Pfeiffer I, Kiricsi M. 2017. Biological activity of green-synthesized silver nanoparticles depends on the applied natural extracts: a comprehensive study. International journal of nanomedicine, 12, 871. DOI 10.2147/IJN.S122842

Salari Z, Danafar F, Dabaghi S, Ataei SA. 2016. Sustainable synthesis of silver nanoparticles using macroalgae *Spirogyra varians* and analysis of their antibacterial activity. Journal of Saudi Chemical Society, 20(4), 459-464. DOI 10.1016/j.jscs.2014.10.004

Shao Y, Jin Y, Dong S. 2004. Synthesis of gold nanoplates by aspartate reduction of gold chloride. Chemical Communications (9), 1104-1105. DOI 10.1039/B315732F

Sharma P, Pant S, Rai S, Yadav RB, Sharma S, Dave V. 2018. Green synthesis and characterization of silver nanoparticles by *Allium cepa* L. to produce silver nano-coated fabric and their antimicrobial evaluation. Applied Organometallic Chemistry, 32(3). DOI 10.1002/aoc.4146

Sharma VK, Yngard RA, Lin Y. 2009. Silver nanoparticles: green synthesis and their antimicrobial activities. Advances in colloid and interface science, 145(1), 83-96. DOI 10.1016/j.cis.2008.09.002

Singh CR, Kathiresan K, Anandhan S. 2015. A review on marine based nanoparticles and their potential applications. African Journal of Biotechnology, 14(18), 1525-1532. DOI 10.5897/AJB2015.14527

Singhal G, Bhavesh R, Kasariya K, Sharma AR, Singh RP. 2011. Biosynthesis of silver nanoparticles using *Ocimum sanctum* (Tulsi) leaf extract and screening its antimicrobial activity. Journal of Nanoparticle Research, 13(7), 2981-2988. DOI 10.1007/s11051-010-0193-y

Sobieh SS, Kheiralla ZMH, Rushdy AA, Yakob NAN. 2016. In vitro and in vivo genotoxicity and molecular response of silver nanoparticles on different biological model systems. Caryologia, 69(2), 147-161. DOI 10.1080/00087114.2016.1139416

Soldini S, Posteraro B, Vella A, De Carolis E, Borghi E, Falleni M, Losito AR, Maiuro G, Trecarichi EM, Sanguinetti, M, Tumbarello M. (2017). Microbiologic and clinical characteristics of biofilm-forming *Candida parapsilosis* isolates associated with fungaemia and their impact on mortality. Clinical Microbiology and Infection. DOI 10.1016/j.cmi.2017.11.005

Sondi I, Siiman O, Koester S, Matijević E. 2000. Preparation of aminodextran– CdS nanoparticle complexes and biologically active antibody– aminodextran– CdS nanoparticle conjugates. Langmuir, 16(7), 3107-3118. DOI 10.1021/la991109r

Suriya J, Raja SB, Sekar V, Rajasekaran R. 2012. Biosynthesis of silver nanoparticles and its antibacterial activity using seaweed *Urospora* sp. African Journal of Biotechnology, 11(58), 12192-12198. DOI 10.5897/AJB12.452

Tippayawat P, Phromviyo N, Boueroy P, Chompoosor A. 2016. Green synthesis of silver nanoparticles in *Aloe vera* plant extract prepared by a hydrothermal method and their synergistic antibacterial activity. PeerJ, 4, e2589. DOI 10.7717/peerj.2589

Travan A, Pelillo C, Donati I, Marsich E, Benincasa M, Scarpa T, Semeraro S, Turco G, Gennaro R, Paoletti, S. 2009. Non-cytotoxic silver nanoparticle-polysaccharide nanocomposites with antimicrobial activity. Biomacromolecules, 10(6), 1429-1435. DOI 10.1021/bm900039x

Vigneshwaran N, Nachane R, Balasubramanya R, Varadarajan P. 2006. A novel one-pot 'green'synthesis of stable silver nanoparticles using soluble starch. Carbohydrate research, 341(12), 2012-2018. DOI 10.1016/j.carres.2006.04.042

Vivek R, Thangam R, Muthuchelian K, Gunasekaran P, Kaveri K, Kannan S. 2012. Green biosynthesis of silver nanoparticles from *Annona squamosa* leaf extract and its in vitro cytotoxic effect on MCF-7 cells. Process Biochemistry, 47(12), 2405-2410. DOI 10.1016/j.procbio.2012.09.025

Wang J, Chen C. 2009. Biosorbents for heavy metals removal and their future. Biotechnology advances, 27(2), 195-226. DOI 10.1016/j.biotechadv.2008.11.002

Zgoda J, Porter J. 2001. A convenient microdilution method for screening natural products against bacteria and fungi. Pharmaceutical Biology, 39(3), 221-225. DOI 10.1076/phbi.39.3.221.5934

Zhang Y, Liu X, Wang Y, Jiang P, Quek S. 2016. Antibacterial activity and mechanism of cinnamon essential oil against *Escherichia coli* and *Staphylococcus aureus*. Food Control, 59, 282-289. DOI 10.1016/j.foodcont.2015.05.032

Zuercher AW, Fritsche R, Corthésy B, Mercenier A. 2006. Food products and allergy development, prevention and treatment. Current opinion in biotechnology, 17(2), 198-203. DOI 10.1016/j.copbio.2006.01.010